

Near-Infrared Dyes

Deutsche Ausgabe: DOI: 10.1002/ange.201511151
Internationale Ausgabe: DOI: 10.1002/anie.201511151A Diradical Approach towards BODIPY-Based Dyes with Intense Near-Infrared Absorption around $\lambda = 1100$ nm

Yong Ni, Sangsu Lee, Minjung Son, Naoki Aratani, Masatoshi Ishida, Animesh Samanta, Hiroko Yamada, Young-Tae Chang, Hiroyuki Furuta, Dongho Kim,* and Jishan Wu*

Abstract: A diradical approach to obtain stable organic dyes with intense absorption around $\lambda = 1100$ nm is reported. The *para*- and *meta*-quinodimethane-bridged BODIPY dimers **BD-1** and **BD-2** were synthesized and were found to have a small amount of diradical character. These molecules exhibited very intense absorption at $\lambda = 1088$ nm ($\epsilon = 6.65 \times 10^5 \text{ M}^{-1} \text{ cm}^{-1}$) and 1136 nm ($\epsilon = 6.44 \times 10^5 \text{ M}^{-1} \text{ cm}^{-1}$), respectively, together with large two-photon-absorption cross-sections. Structural isomerization induced little variation in their diradical character but distinctive differences in their physical properties. Moreover, the compounds showed a selective fluorescence turn-on response in the presence of the hydroxyl radical but not with other reactive oxygen species.

Organic dyes with strong absorption in the near-infrared (NIR) region of the electromagnetic spectrum have found practical application in photonics, electronics, and bio-imaging.^[1] Conventional design principles for NIR dyes have mainly included the extension of π conjugation and the introduction of a push–pull motif, and employing these strategies many stable NIR dyes have been synthesized. However, only very few examples of stable organic dyes with intense absorption beyond $\lambda = 1000$ nm have been reported,^[2] a property especially useful for Nd:YAG $\lambda = 1064$ nm laser protection and optical switching at telecommunication-appro-

priate wavelengths. By using the conventional strategy, a largely delocalized system has to be designed in order to obtain a material with a very small HOMO–LUMO energy gap, which is synthetically challenging. Our group and others recently demonstrated that certain type of pro-aromatic and antiaromatic π -conjugated molecules existed as singlet diradicals in the ground state and exhibited small energy gaps,^[3] thus they could be good candidates for organic NIR dyes. However, these diradicaloids suffered from an intrinsic instability resulting from their distinctive diradical character. Fabian et al. previously discussed the role of the diradical character on the design of NIR dyes,^[4] but this was not well-developed mainly because of the lack of appropriate design rules and synthetic strategies for stable diradicaloids. Given the tremendous development of diradicaloids in recent years, we believe that it is time to revisit the diradical approach for the design of NIR dyes.

Our strategy involves the construction of *para*- and *meta*-quinodimethane (*p*-QDM and *m*-QDM) bridged BODIPY dimers **BD-1** and **BD-2** (Figure 1; BODIPY = boron-dipyrromethene). BODIPY was chosen as the main building block mainly because of its excellent stability arising from the strongly electron-withdrawing BF_2 group, as well as for its intense absorption.^[5] Although many BODIPY-based NIR dyes have been synthesized,^[6] their absorption bands mostly fall in the range of $\lambda = 700$ – 900 nm. Incorporation of a *p*-QDM or *m*-QDM into the π -conjugated BODIPY dimer framework would lead to new stable dyes with an even smaller energy gap resulting from the occurrence of diradical character. Both **BD-1** and **BD-2** can be regarded as diradicaloids because of their pro-aromatic character and the aromatic stabilization of the diradical form (Figure 1).

[*] Dr. Y. Ni, Prof. Dr. J. Wu

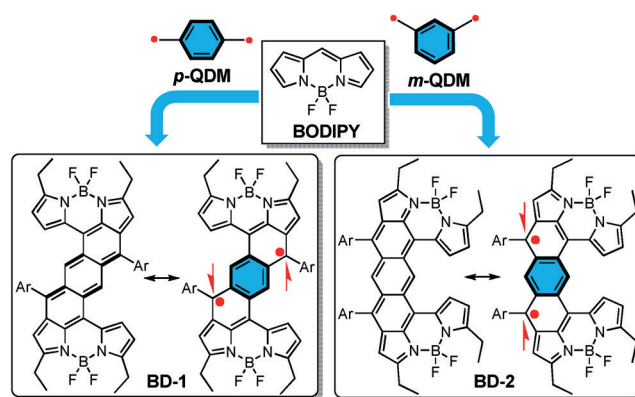
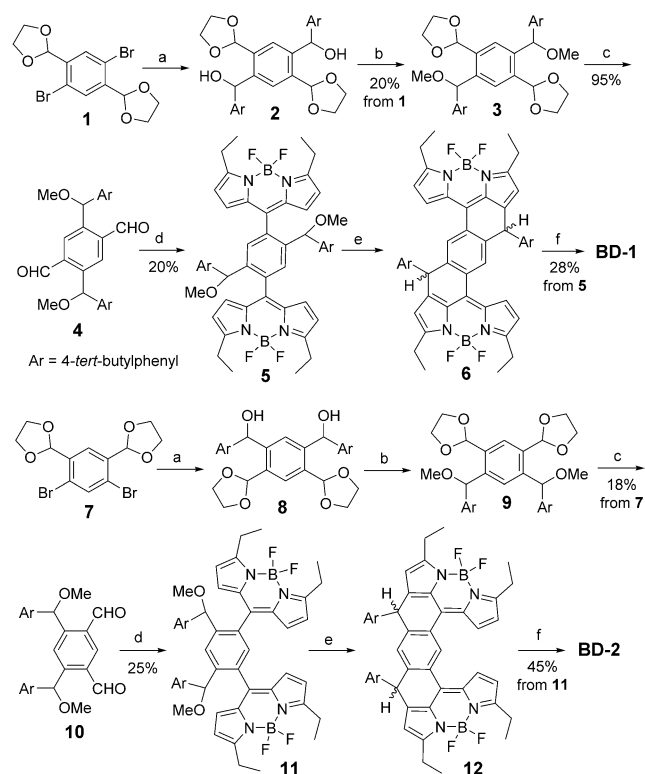
Department of Chemistry, National University of Singapore
117543 Singapore (Singapore)
E-mail: chmwuj@nus.edu.sgS. Lee, M. Son, Prof. Dr. D. Kim
Spectroscopy Laboratory for Functional π -Electronic Systems and
Department of Chemistry, Yonsei University
Seoul 120-749 (Korea)Prof. Dr. N. Aratani, Prof. Dr. H. Yamada
Graduate School of Materials Science
Nara Institute of Science and Technology
8916-5 Takayama-cho, Ikoma 630-0192 (Japan)M. Ishida, Prof. Dr. H. Furuta
Education Center for Global Leaders in Molecular Systems for
Devices, Kyushu University
744 Motooka, Nishi-ku, Fukuoka 819-0395 (Japan)Dr. Y. Ni, Dr. A. Samanta, Prof. Dr. Y.-T. Chang
Laboratory of Bioimaging Probe Development
Singapore Bioimaging Consortium, 138667 Singapore (Singapore)Prof. Dr. J. Wu
Institute of Materials Research and Engineering, A*STAR
2 Fusionopolis Way, Innovis, #08-03, 117602 Singapore (Singapore)Supporting information for this article is available on the WWW
under <http://dx.doi.org/10.1002/anie.201511151>.

Figure 1. The structures of *p*-QDM, *m*-QDM, and their bridged BODIPY dimers **BD-1** and **BD-2**. Ar = 4-*tert*-butylphenyl.

Indeed, both molecules have a small amount of diradical character and exhibit very intense one-photon absorption (OPA) around $\lambda = 1100$ nm and large two-photon-absorption (TPA) cross-sections in the NIR region. The effect of the structural isomerization on the diradical character and consequently their physical properties was also discussed. Moreover, the potential of these molecules for selective detection, by means of fluorescence turn-on, for the hydroxyl radical ($\cdot\text{OH}$) over other reactive oxygen species (ROS) was tested.

The synthesis of **BD-1** and **BD-2** is shown in Scheme 1. Lithiation of ethylene glycol protected dibromophenylaldehydes **1**^[7] and **7**^[8] followed by reaction with 4-*tert*-butylbenzaldehyde afforded the corresponding diols **2** and **8**. After methylation and acid-promoted deprotection, the dialdehydes **4** and **10** were obtained. Compounds **4** and **10** were subjected to trifluoroacetic acid (TFA) catalyzed condensation with 2-ethylpyrrole, oxidation with 2,3-dichloro-5,6-dicyano-1,4-benzoquinone (DDQ), and complexation with $\text{BF}_3 \cdot \text{OEt}_2$ to give the BODIPY dimers **5** and **11**. Then cyclization of **5** and **11** promoted by $\text{BF}_3 \cdot \text{OEt}_2$ gave the corresponding BODIPY dimers **6** and **12** and subsequent dehydrogenation by DDQ finally afforded the fully-conjugated BODIPY dimers **BD-1** and **BD-2** as dark-green solids.

Both **BD-1** and **BD-2** are very stable both solution and in the solid state under ambient conditions. An X-ray crystallo-



Scheme 1. Synthesis of **BD-1** and **BD-2**. Reagents and conditions: a) *n*-BuLi, THF, -78°C , 2 h; Ar-CHO, -78°C to RT, overnight; b) NaH, MeI, THF/DMF (4:1 v/v), 0°C to RT; c) *p*-toluenesulfonic acid, acetone/ H_2O (2:1 v/v), reflux for 6 h; d) i) 2-ethylpyrrole, TFA, DCM, RT, 3 h; ii) DDQ, DCM, 2 h; iii) TEA, $\text{BF}_3 \cdot \text{OEt}_2$, DCM, RT, 0.5 h; e) $\text{BF}_3 \cdot \text{OEt}_2$, DCM, 20 min; f) DDQ, DCM, 0.5 h. TEA = triethylamine; DCM = dichloromethane.

graphic analysis (Figure 2a,b)^[9] revealed a significant distortion angle (11.7° for **BD-1** and 13.3° for **BD-2**) resulting from steric congestion between the BODIPY subunits and the central benzene ring. **BD-1** has a centrally symmetric structure and the molecules are stacked into 1D columnar structure through both π - π interactions (average distance = 3.386 \AA) and dipole-dipole interactions. In contrast, **BD-2** has a helical structure and the *p*- and *m*-enantiomers are packed into a 1D chain-like structure in an alternating mode by means of multiple $[\text{C}-\text{H} \cdots \pi]/[\text{C}-\text{H} \cdots \text{F}]$ and dipole-dipole interactions (see Figure S1 in the Supporting Information). Both molecules can be drawn in three major resonance forms (Figure 2c): a closed-shell dipyrrole-substituted antiaromatic

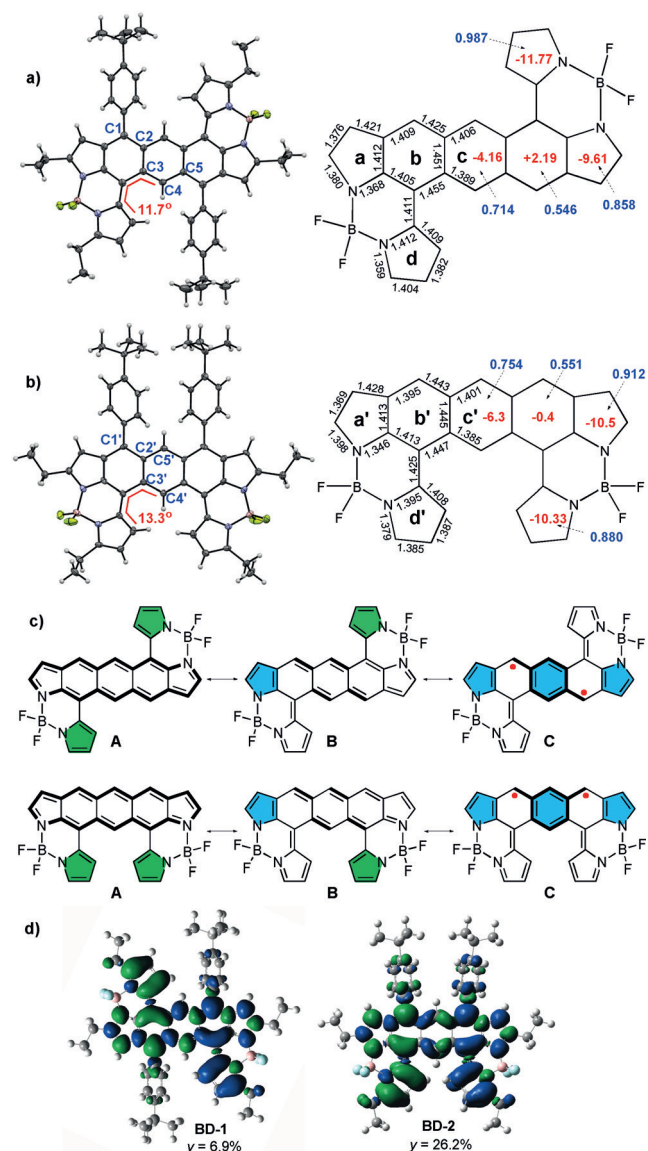


Figure 2. ORTEP representations and mean bond lengths (\AA) for the crystal structures of a) **BD-1** and b) **BD-2**. The red and blue numbers are the calculated NICS(1)_{zz} and HOMA values of the selected rings, respectively. c) Different resonance forms for **BD-1** and **BD-2**. The blue and green surfaces represent α and β spin densities, respectively. d) Calculated (UB3LYP/6-31G*) spin density distributions of **BD-1** and **BD-2** in the singlet diradical form.

(20 π electron) benzo[1,2-*f*:4,5-*f'*]diindole (for **BD-1**) or benzo[1,2-*f*:5,4-*f'*]diindole (for **BD-2**) form A, a closed-shell quinoidal form B, and an open-shell diradical form C. Although the steric-strain-induced nonplanarity further complicates the bond-length analysis, an obvious bond-length alternation (BLA) in the central *p*-QDM subunit in **BD-1** was detected (C1–C2 = 1.425 Å; C2–C3 = 1.451 Å; C3–C4 = 1.389 Å; C4–C5 = 1.406 Å), indicating that closed-shell forms A and B were the major contributions to the structure. However, the C1–C2 bond length (1.425 Å) is much longer than that of a typical double bond in olefins (1.33–1.34 Å), indicating significant contribution of the diradical form to the ground state. Similarly, **BD-2** also showed obvious BLA in the QDM subunit (C1'–C2' = 1.443 Å; C2'–C3' = 1.445 Å; C3'–C4' = 1.385 Å; C2'–C5' = 1.401 Å). However, the C1'–C2' bond length is longer than that of C1–C2 in **BD-1** and the BLA in the central benzene ring is smaller than that in **BD-1**, indicating a larger contribution of the diradical form to the ground state.

The diradical character (y) of **BD-1** and **BD-2** were estimated to be 6.9% and 26.2% at the UB3LYP/6-31G* level of theory, respectively. Calculations also predicted that the spins are delocalized onto the whole π -conjugated framework, with large spin density at the carbon centers linking the 4-*tert*-butylphenyl substituents (Figure 2d). However, experimentally, both **BD-1** and **BD-2** showed sharp NMR signals even at elevated temperatures and there was no detectable ESR signal in solution and in the powder state, indicating that there is a small amount of diradical character in both cases. Nucleus independent chemical shift (NICS)^[10] calculations at the center of a ring for the optimized structures of both isomers revealed more negative NICS(1)_{zz} values for ring c' (−6.3 ppm), ring b' (−0.4 ppm), and ring a' (−10.5 ppm) in **BD-2** than the corresponding ring c (−4.16 ppm), b (+2.19 ppm), and a (−9.6 ppm) in **BD-1**, indicative of the larger aromatic character of these rings in **BD-2** and thus a larger contribution of the diradical form in **BD-2**. In addition, harmonic oscillator model of aromaticity (HOMA) analysis on each individual ring also support this conclusion (Figure 2a,b; values given in blue).

BD-1 and **BD-2** exhibited strong absorption bands at $\lambda = 1088$ nm ($\epsilon = 6.65 \times 10^5 \text{ M}^{-1} \text{ cm}^{-1}$; full width at half maximum (fwhm) = 70 nm) and 1136 nm ($\epsilon = 6.44 \times 10^5 \text{ M}^{-1} \text{ cm}^{-1}$; fwhm = 94 nm), respectively (Figure 3). Compounds **BD-1** and **BD-2** are also fluorescent, having emission maxima at $\lambda = 1120$ nm (quantum yield $\Phi = 0.2\%$) and 1193 nm ($\Phi = 0.02\%$), respectively (Figure S2). On the basis of these values, optical energy gaps of 0.80 eV and 0.79 eV, respectively, could then be roughly estimated. Both isomers display well-resolved multiple-stage amphoteric redox waves in their cyclic voltammograms (**BD-1**: $E_{1/2}^{\text{ox}} = 0.52, 0.85, 1.22$ V; $E_{1/2}^{\text{red}} = -0.37, -0.72$ V; **BD-2**: $E_{1/2}^{\text{ox}} = 0.55, 0.70, 0.89, 1.21$ V; $E_{1/2}^{\text{red}} = -0.29, -0.66$ V; values quoted versus Fc/Fc⁺; Figure S3 and Table S1). The estimated electrochemical energy gaps ($E_g^{\text{EC}} = 0.75$ eV for **BD-1**, 0.72 eV for **BD-2**) are consistent with the optical energy gaps. Compared with other typical closed-shell π -conjugated systems, such as a benzo-[*b*]-fused BODIPY dimer ($\lambda_{\text{max}}^{\text{abs}} = 629$ nm, $\epsilon = 1.02 \times 10^5 \text{ M}^{-1} \text{ cm}^{-1}$),^[11] a benzo-[*a*]-fused BODIPY dimer

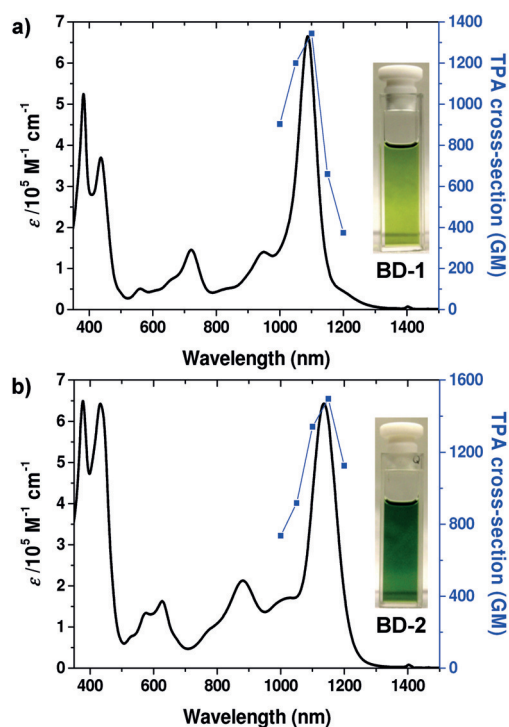


Figure 3. One-photon absorption spectra (black line, left vertical axis) and TPA spectra (blue symbols, right vertical axis) of a) **BD-1** and b) **BD-2**. TPA spectra are plotted at $\lambda_{\text{ex}}/2$. Inset: photographs of solutions of the compounds in chloroform.

($\lambda_{\text{max}}^{\text{abs}} = 758$ nm, $\epsilon = 1.9 \times 10^5 \text{ M}^{-1} \text{ cm}^{-1}$),^[12] and a *p*-QDM-bridged porphyrin dimer ($\lambda_{\text{max}}^{\text{abs}} = 955$ nm, $\epsilon = 4.54 \times 10^4 \text{ M}^{-1} \text{ cm}^{-1}$),^[13] **BD-1** and **BD-2** showed bathochromic shifts of nearly 500 nm, 350 nm, and 150 nm, respectively, despite their similar π -conjugation size. Dyes **BD-1** and **BD-2** are rare examples of NIR dyes with very intense absorption around $\lambda = 1100$ nm and may find practical application in Nd:YAG 1064 nm laser protection.

Short singlet excited-state lifetimes were estimated for both **BD-1** ($\tau = 25.7$ ps) and **BD-2** ($\tau = 22$ ps) from femto-second transient absorption (TA) measurements (Figure S4–5). These short lifetimes indicate a fast nonradiative internal conversion process arising from a small energy gap, which also explains their weak fluorescence. Recent theoretical studies indicated that small and moderate amounts of diradical character may be important for TPA enhancement.^[14] Indeed, large TPA cross-section values were obtained for both **BD-1** ($\sigma_{\text{max}}^{(2)} = 1300$ GM at $\lambda = 2200$ nm) and **BD-2** ($\sigma_{\text{max}}^{(2)} = 1500$ GM at $\lambda = 2300$ nm) in the NIR region (Figure 3; Figure S6). It was also noted that structural isomerization of **BD-1** and **BD-2** resulted in a variation of their diradical character and consequently their physical properties, that is, the *m*-QDM-bridged BODIPY dimer **BD-2** with greater diradical character exhibited a longer-wavelength absorption maximum, a larger TPA cross-section, a lower fluorescence quantum yield, and a shorter singlet excited-state lifetime than the *p*-QDM-bridged BODIPY dimer **BD-1**.

The non-negligible diradical character of **BD-1** and **BD-2** implies that they may selectively react with reactive oxygen

species (ROS), which play crucial roles in pathological effects, aging, cellular disorders, and cytotoxic effects.^[15] To test this concept, both **BD-1** and **BD-2** were treated with various ROS. It was found that both dyes displayed dramatic selective fluorescence enhancements at around $\lambda = 650$ nm (40-fold for **BD-1**, 100-fold for **BD-2**) for the hydroxyl radical over other ROS (Figure 4; Figure S7), and that the fluorescence intensity is proportional to the concentration of the hydroxyl radical (Figure S8). The increase in the intensity of the fluorescence

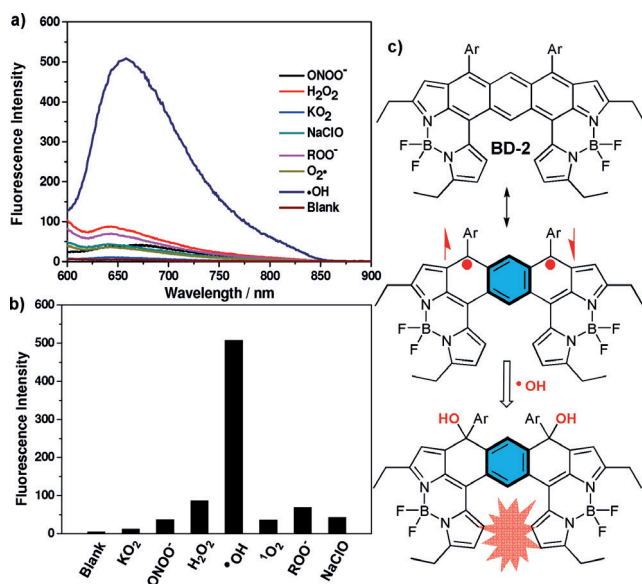


Figure 4. a) Fluorescence spectra of **BD-2** after addition of 20 equiv. of various reactive oxygen species. b) Comparison of fluorescent response of **BD-2** to various ROS. c) Proposed mechanism for the fluorescence turn-on response to the hydroxyl radical.

and the significant blue-shift that it has undergone can be attributed to the radical additive reaction to the *p*-QDM/*m*-QDM-bridged BODIPY dimer backbone and the conjugation disruption, as confirmed by mass spectrometry measurements (Figure S9–11). The similarities of the UV/Vis/NIR absorption and emission spectra of the resulting solution to those of the corresponding *p*- and *m*-phenyl-bridged BODIPY dimers **6** and **12** (Figure S11) suggested that the hydroxyl groups are mainly attached to the carbon centers linking the 4-*tert*-butylphenyl groups. On the other hand, KO_2 and ONOO^- induced a significant red-shift of the absorption maximum from around $\lambda = 1100$ nm to 1500 nm for both isomers, which is likely due to formation of radical cation species (Figure S12–13).

In summary, structurally isomeric *p*-QDM and *m*-QDM-bridged BODIPY dimers **BD-1** and **BD-2** were synthesized. Both compounds showed good stability towards oxidation in air because of the electron-withdrawing BF_2 units. These molecules had a small amount of diradical character and the intermediate coupling between the frontier two spins led to NIR dyes with very intense one-photon absorption around $\lambda = 1100$ nm and large TPA cross-sections in the NIR region. It was also found that a small amount of variation in the

diradical character significantly affected their physical properties. Our studies provided insight into the design of NIR dyes using a new diradical concept. Diradicaloids with a small or moderate amount of diradical character could be good NIR dyes if appropriately stabilized. Moreover, we also carried out a proof-of-concept study using diradicaloids for the selective fluorescence turn-on detection of ROS.

Acknowledgements

This work was supported by the MOE Tier 3 programme (MOE2014-T3-1-004) and an A*STAR JCO grant (1431AFG100). The work at Yonsei University was supported by the Mid-Career Researcher Program (NRF-2005-0093839) and the Global Research Laboratory (2013K1A1A2A02050183) through the National Research Foundation of Korea (NRF) funded by the Ministry of Science, ICT (Information and Communication Technologies), and Future Planning.

Keywords: BODIPY · dyes/pigments · fluorescence · radicals · reactive oxygen species

How to cite: *Angew. Chem. Int. Ed.* **2016**, *55*, 2815–2819
Angew. Chem. **2016**, *128*, 2865–2869

- [1] a) J. Fabian, H. Nakanzumi, M. Matsuoka, *Chem. Rev.* **1992**, *92*, 1197; b) G. Qian, Z. Wang, *Chem. Asian J.* **2010**, *5*, 1006; c) A. Muranaka, M. Yonehara, M. Uchiyama, *J. Am. Chem. Soc.* **2010**, *132*, 7844; d) G. M. Fischer, E. Daltrozzi, A. Zumbusch, *Angew. Chem. Int. Ed.* **2011**, *50*, 1406; *Angew. Chem.* **2011**, *123*, 1442.
- [2] a) T. P. Simard, J. H. Yu, J. M. Zebrowski-Young, N. F. Haley, M. R. Detty, *J. Org. Chem.* **2000**, *65*, 2236; b) A. Tsuda, A. Osuka, *Science* **2001**, *293*, 79; c) T. Ikeda, N. Aratani, A. Osuka, *Chem. Asian J.* **2009**, *4*, 1248; d) M. Tian, S. Tatsuura, M. Furuki, Y. Sato, I. Iwasa, L. Pu, *J. Am. Chem. Soc.* **2003**, *125*, 348; e) Z. Yuan, S. L. Lee, L. Chen, C. Li, K. S. Mali, S. de Feyter, K. Müllen, *Chem. Eur. J.* **2013**, *19*, 11842; f) J. Luo, S. Lee, M. Son, B. Zheng, K.-W. Huang, Q. Qi, W. Zeng, G. Li, D. Kim, J. Wu, *Chem. Eur. J.* **2015**, *21*, 3708.
- [3] a) Z. Sun, Q. Ye, C. Chi, J. Wu, *Chem. Soc. Rev.* **2012**, *41*, 7857; b) A. Shimizu, Y. Hirao, T. Kubo, M. Nakano, E. Botek, B. Champagne, *AIP Conf. Proc.* **2012**, *1504*, 399; c) Z. Sun, Z. Zeng, J. Wu, *Chem. Asian J.* **2013**, *8*, 2894; d) M. Abe, *Chem. Rev.* **2013**, *113*, 7011; e) Z. Sun, Z. Zeng, J. Wu, *Acc. Chem. Res.* **2014**, *47*, 2582; f) T. Kubo, *Chem. Rec.* **2015**, *15*, 218; g) Z. Zeng, X. L. Shi, C. Chi, J. T. López Navarrete, J. Casado, J. Wu, *Chem. Soc. Rev.* **2015**, *44*, 6578.
- [4] a) J. Fabian, R. Zahradník, *Angew. Chem. Int. Ed. Engl.* **1989**, *28*, 677; *Angew. Chem.* **1989**, *101*, 693; b) J. Fabian, R. Peichert, *J. Phys. Org. Chem.* **2010**, *23*, 1137.
- [5] a) A. Loudet, K. Burgess, *Chem. Rev.* **2007**, *107*, 4891; b) G. Ulrich, R. Ziessel, A. Harriman, *Angew. Chem. Int. Ed.* **2008**, *47*, 1184; *Angew. Chem.* **2008**, *120*, 1202; c) N. Boens, V. Leen, W. Dehaen, *Chem. Soc. Rev.* **2012**, *41*, 1130; d) J. Ahrens, B. Haberland, A. Scheja, M. Tamm, M. Bröring, *Chem. Eur. J.* **2014**, *20*, 2901; e) D. Frath, J. Massue, G. Ulrich, R. Ziessel, *Angew. Chem. Int. Ed.* **2014**, *53*, 2290; *Angew. Chem.* **2014**, *126*, 2322; f) T. Kowada, H. Maeda, K. Kikuchi, *Chem. Soc. Rev.* **2015**, *44*, 4953; g) T. Bruhn, G. Pescitelli, S. Jurinovich, A. Schaumlöfel, F. Witterauf, J. Ahrens, M. Bröring, G. Bringmann, *Angew. Chem. Int. Ed.* **2014**, *53*, 14592; *Angew. Chem.* **2014**, *126*, 14821.

- [6] a) W. Zhao, E. M. Carreira, *Angew. Chem. Int. Ed.* **2005**, *44*, 1677; *Angew. Chem.* **2005**, *117*, 1705; b) K. Umezawa, Y. Nakamura, H. Makino, D. Citterio, K. Suzuki, *J. Am. Chem. Soc.* **2008**, *130*, 1550; c) A. Matsui, K. Umezawa, Y. Shindo, T. Fujii, D. Citterio, K. Oka, K. Suzuki, *Chem. Commun.* **2011**, 47, 10407; d) C. Jiao, K.-W. Huang, J. Wu, *Org. Lett.* **2011**, *13*, 632; e) Y. Hayashi, N. Obata, S. Seki, Y. Kureishi, S. Saito, S. Yamaguchi, H. Shinokubo, *Org. Lett.* **2012**, *14*, 866; f) Y. Ni, W. Zeng, K. Huang, J. Wu, *Chem. Commun.* **2013**, 49, 1217; g) J. Wang, Q. Wu, S. Wang, C. Yu, J. Li, E. Hao, Y. Wei, X. Mu, L. Jiao, *Org. Lett.* **2015**, *17*, 5360.
- [7] Z. Xie, B. Yang, L. Liu, M. Li, D. Lin, Y. Ma, G. Cheng, S. Liu, *J. Phys. Org. Chem.* **2005**, *18*, 962.
- [8] T. Itoh, T. Maemura, Y. Ohtsuka, Y. Ikari, H. Wildt, K. Hirai, H. Tomioka, *Eur. J. Org. Chem.* **2004**, 2991.
- [9] a) Crystallographic data for **BD-1** (103(2) K): $C_{54}H_{54}B_2F_4N_4$, $M_w = 856.63$; monoclinic; space group $P2_1/n$; $a = 9.3333(3)$ Å, $b = 14.5977(4)$ Å, $c = 16.0008(4)$ Å, $\alpha = 90^\circ$, $\beta = 105.782(7)^\circ$, $\gamma = 90^\circ$; $V = 2097.85(12)$ Å³; $Z = 2$; $\rho_{\text{calcd}} = 1.356$ Mg m⁻³; $R1 = 0.0535$, $wR2 = 0.1082$ ($I > 2\sigma(I)$); $R1 = 0.0865$, $wR2 = 0.1196$ (all data). b) Crystallographic data for **BD-2** (90 K): $C_{54}H_{54}B_2F_4N_4$, $M_w = 856.63$; monoclinic; space group $I2/a$; $a = 10.506(7)$ Å, $b = 19.905(14)$ Å, $c = 21.084(14)$ Å, $\alpha = 90^\circ$, $\beta = 96.936(13)^\circ$, $\gamma = 90^\circ$; $V = 4377(5)$ Å³; $Z = 4$; $\rho_{\text{calcd}} = 1.300$ Mg m⁻³; $R1 = 0.1186$, $wR2 = 0.2931$ ($I > 2\sigma(I)$); $R1 = 0.1749$, $wR2 = 0.3408$ (all data). CCDC 1447856 (**BD-1**) and 1447855 (**BD-2**) contain the supplementary crystallographic data for this paper. These data are provided free of charge by The Cambridge Crystallographic Data Centre.
- [10] H. Fallah-Bagher-Shaidaei, C. S. Wannere, C. Corminboeuf, R. Puchta, P. v. R. Schleyer, *Org. Lett.* **2006**, *8*, 863.
- [11] M. Nakamura, H. Tahara, K. Takahashi, T. Nagata, H. Uoyama, D. Kuzuhara, S. Mori, T. Okujima, H. Yamada, H. Uno, *Org. Biomol. Chem.* **2012**, *10*, 6840.
- [12] A. Wakamiya, T. Murakami, S. Yamaguchi, *Chem. Sci.* **2013**, *4*, 1002.
- [13] W. Zeng, M. Ishida, S. Lee, Y. Sung, Z. Zeng, Y. Ni, C. Chi, D. Kim, J. Wu, *Chem. Eur. J.* **2013**, *19*, 16814.
- [14] a) M. Nakano, R. Kishi, S. Ohta, H. Takahashi, T. Kubo, K. Kamada, K. Ohta, E. Botek, B. Champagne, *Phys. Rev. Lett.* **2007**, *99*, 033001; b) K. Yoneda, M. Nakano, Y. Inoue, T. Inui, K. Fukuda, Y. Shigeta, T. Kubo, B. Champagne, *J. Phys. Chem. C* **2012**, *116*, 17787.
- [15] a) J. M. McCord, *Science* **1974**, *185*, 529; b) V. L. Johnson, L. M. Walsh, B. L. Chen, *Proc. Natl. Acad. Sci. USA* **1980**, *77*, 990; c) M. K. Shigenaga, T. M. Hagen, B. N. Ames, *Proc. Natl. Acad. Sci. USA* **1994**, *91*, 10771; d) K. N. Schmidt, P. Amstad, P. Cerutti, P. A. Baeuerle, *Chem. Biol.* **1995**, *2*, 13; e) H. Wiseman, B. Halliwell, *Biochem. J.* **1996**, *313*, 17; f) A. P. De Silva, H. Q. N. Gunaratne, T. Gunnlaugsson, A. J. M. Huxley, C. P. McCoy, J. T. Rademacher, T. E. Rice, *Chem. Rev.* **1997**, *97*, 1515; g) K. Dobashi, B. Ghosh, J. K. Orak, I. Singh, A. K. Singh, *Mol. Cell. Biol.* **2000**, *205*, 1.

Received: December 1, 2015

Published online: January 25, 2016